Supporting Information

Dual function of precisely modified hydroxy-PS-*b*-PMMA as neutral layers and thin films for perpendicularly oriented lamella

Riku Mizusaki,[a] Shinsuke Maekawa,[a] Takehiro Seshimo,[b] Takahiro Dazai,[b] Kazufumi Sato,[b] Kan Hatakeyama-Sato,[a] Yuta Nabae[a] and Teruaki Hayakawa[a*]

*Corresponding author Email: hayakawa.t.ac@m.titech.ac.jp

[a] School of Materials and Chemical Technology, Tokyo Institute of Technology, 2-12-S8-36 Ookayama, Meguro-ku, Tokyo, Japan.

[b] TOKYO OHKA KOGYO CO., LTD., 1590 Tabata, Samukawa-machi, Koza-gun, Kanagawa, Japan.

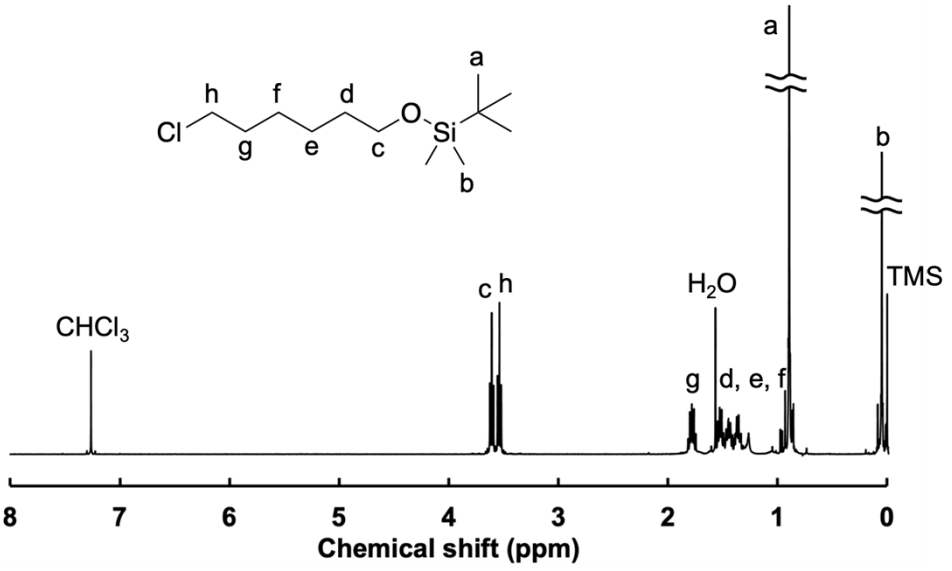

Fig. S1 ^{1}H NMR spectrum of ClC_6OTBS in $CDCl_3$.[1]

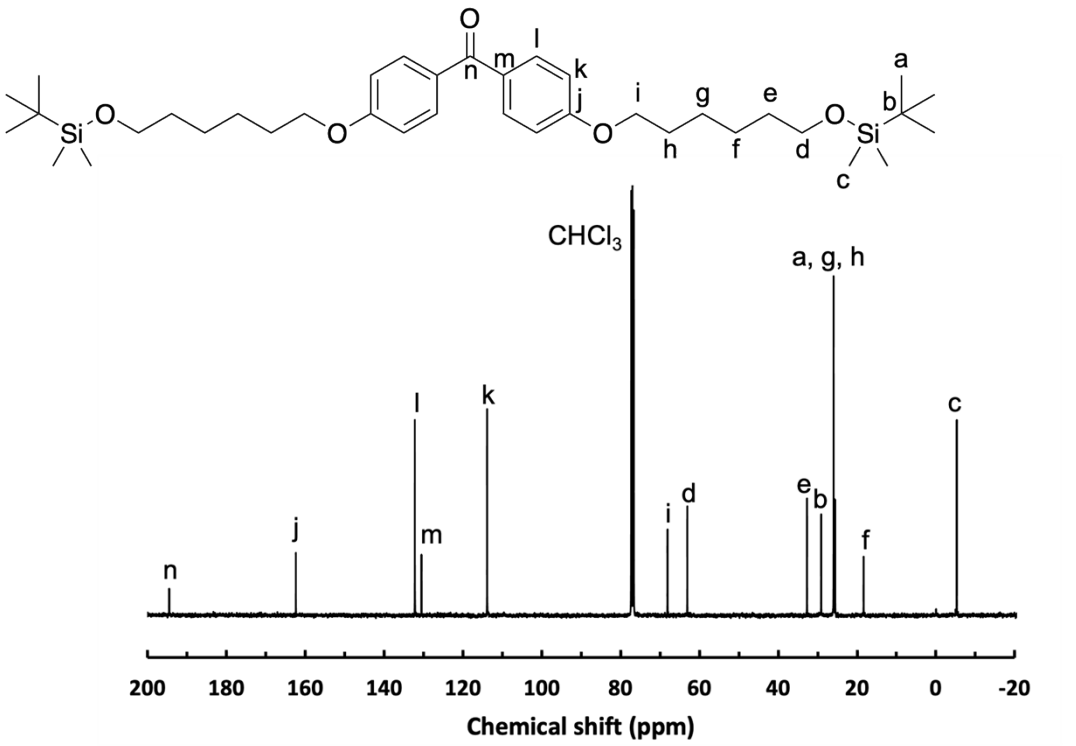

Fig. S2 ^{1}H NMR spectrum of BP-$(OTBS)_2$ in $CDCl_3$.

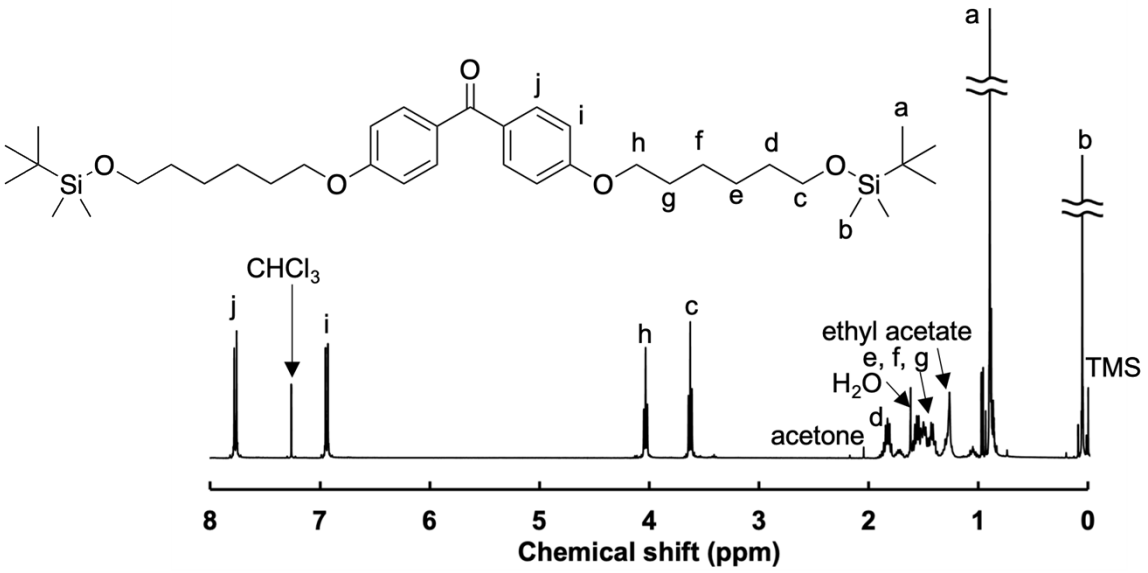

Fig. S3 ^{13}C NMR spectrum of BP-$(OTBS)_2$ in $CDCl_3$.

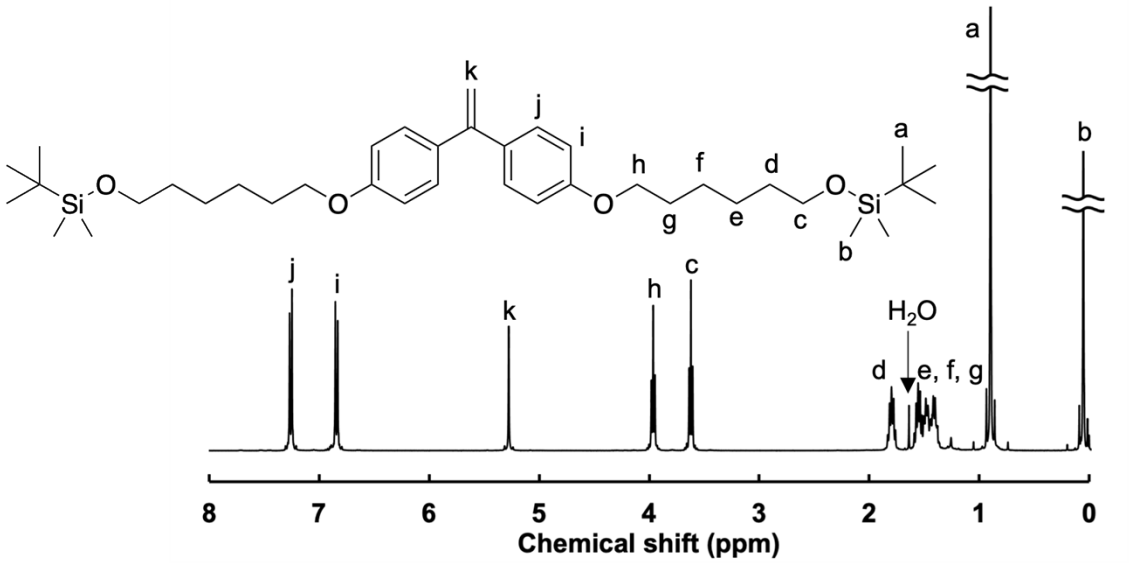

Fig. S4 ^{1}H NMR spectrum of DPE-$(OTBS)_2$ in $CDCl_3$.

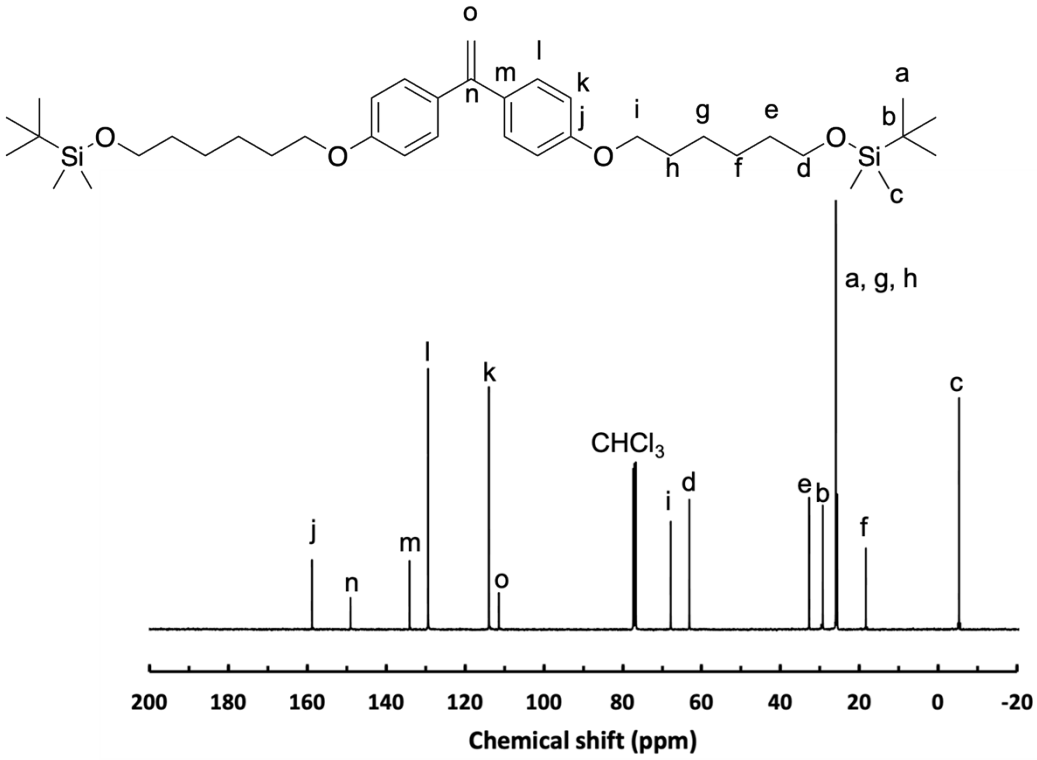

Fig. S5 ^{13}C NMR spectrum of DPE-$(OTBS)_2$ in $CDCl_3$.

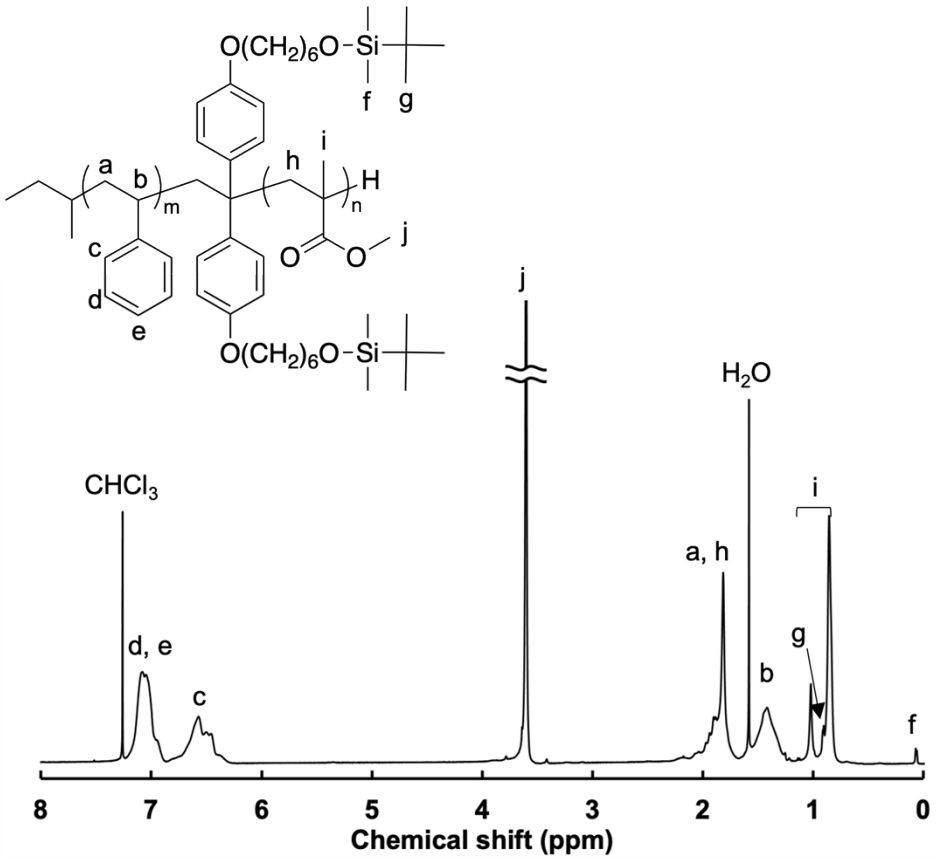

Fig. S6 ^{1}H NMR spectrum of PS-$(OTBS)_2$-PMMA in $CDCl_3$ without TMS.

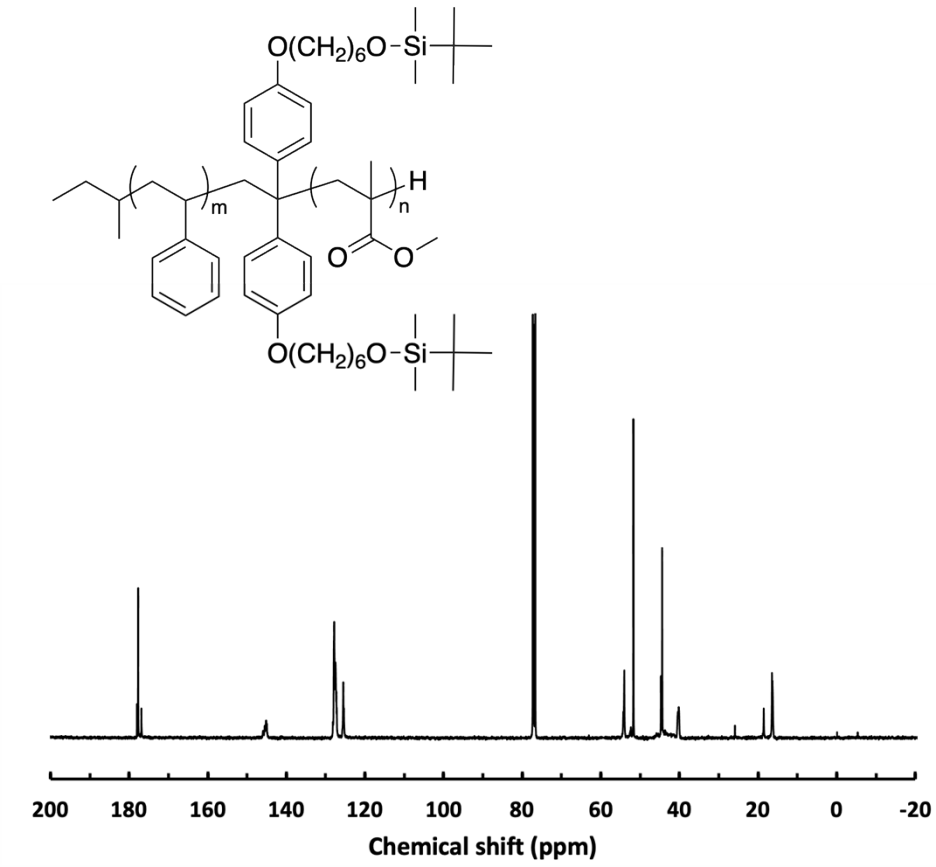

Fig. S7 ^{13}C NMR spectrum of PS-$(OTBS)_2$-PMMA in $CDCl_3$.

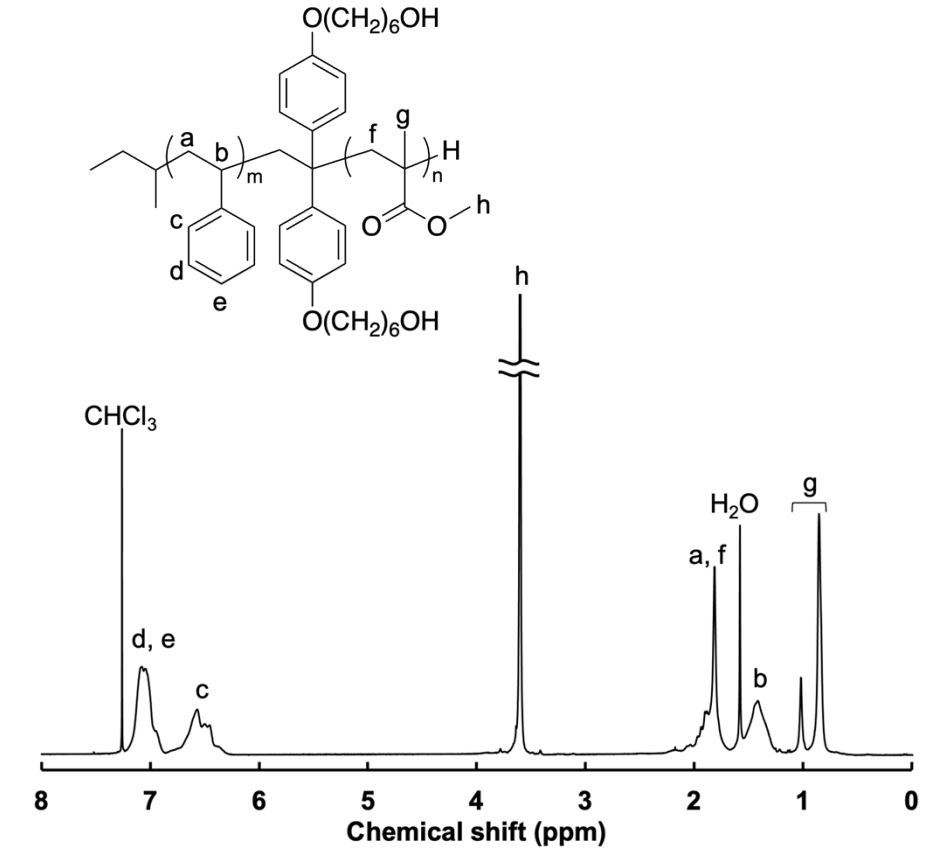

Fig. S8 ^{1}H NMR spectrum of PS-$(OH)_2$-PMMA in $CDCl_3$ without TMS.

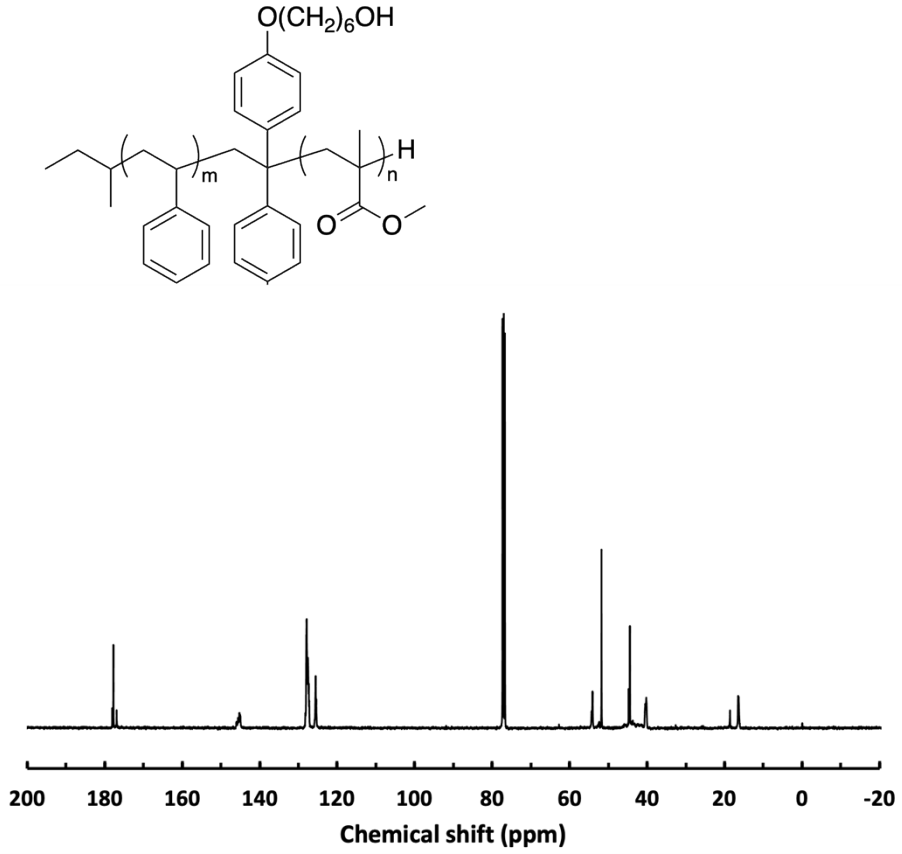

Fig. S9 ^{13}C NMR spectrum of PS-$(OH)_2$-PMMA in $CDCl_3$.

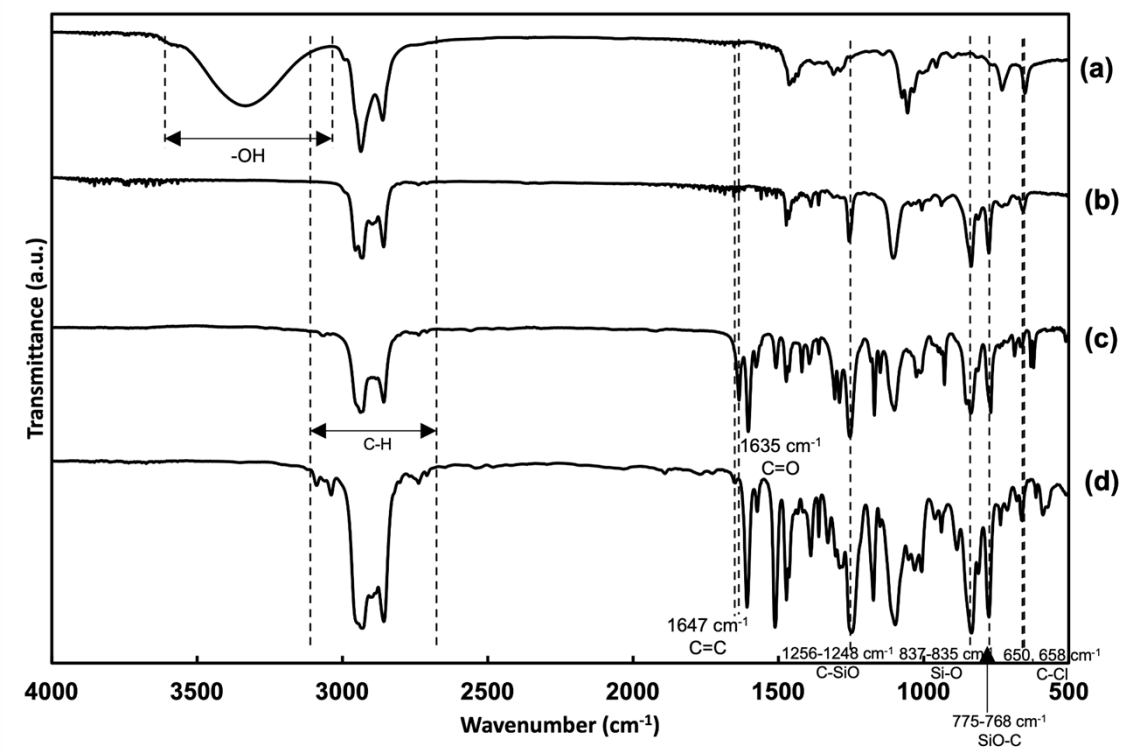

Fig. S10 FT-IR spectra of (a) 6-chloro-1-hexanol, (b) ClC_6OTBS, (c) BP-$(OTBS)_2$ and (d) DPE-$(OTBS)_2$.

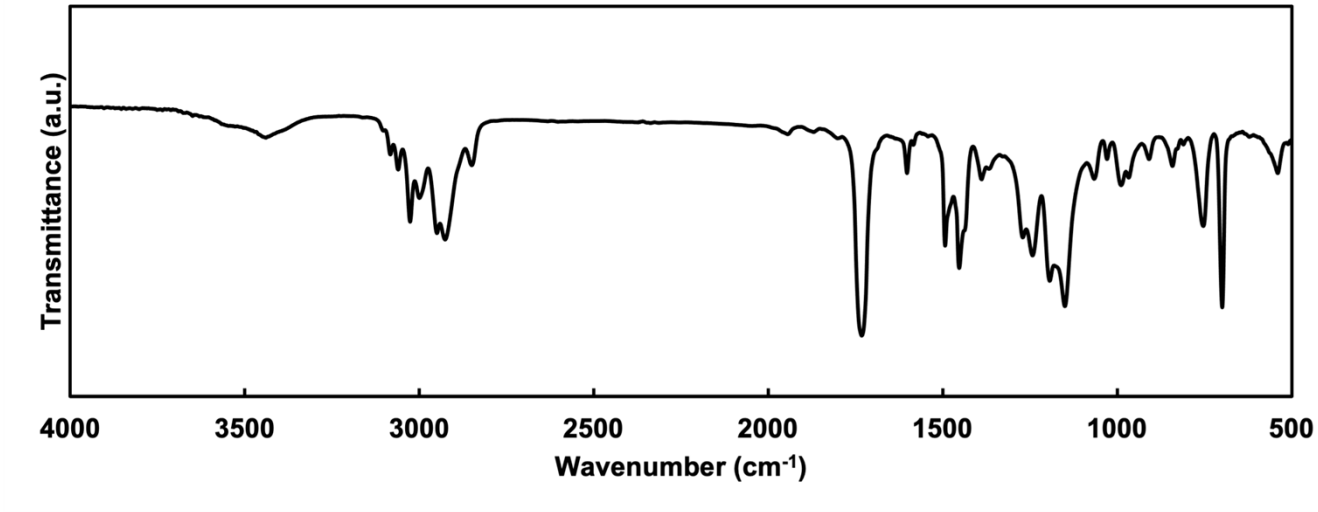

Fig. S11 FT-IR spectrum of PS-$(OTBS)_2$-PMMA.

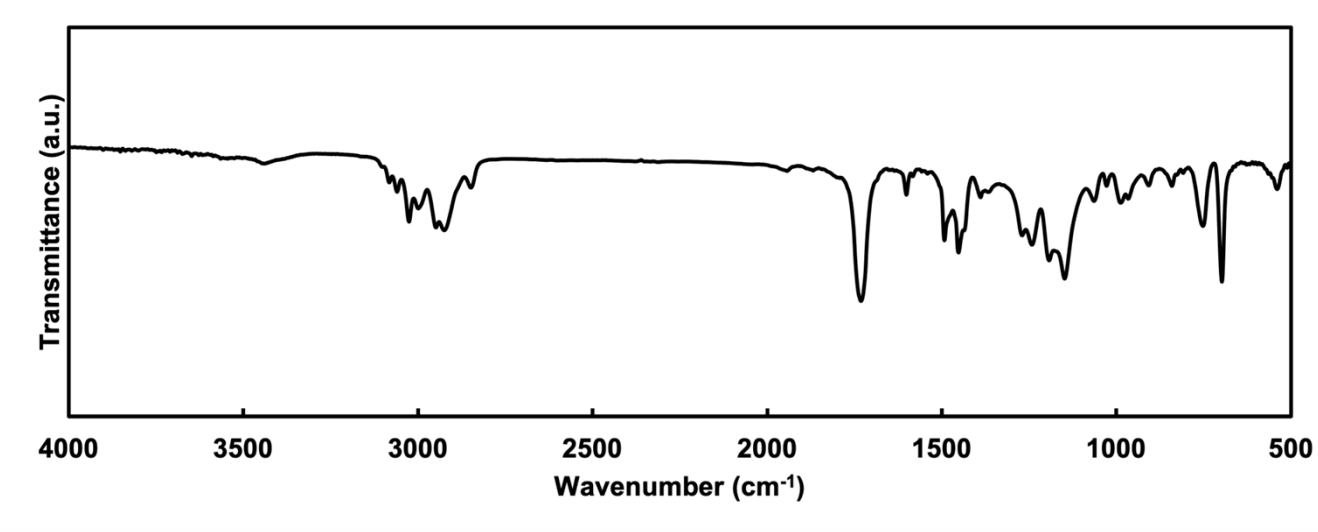

Fig. S12 FT-IR spectrum of PS-$(OH)_2$-PMMA.

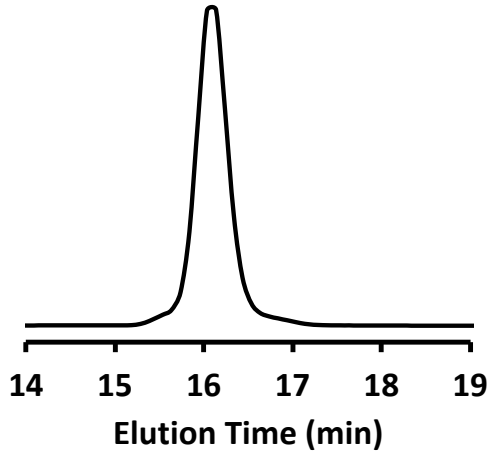

Fig. S13 SEC chromatogram of PS-$(OTBS)_2$-PMMA.

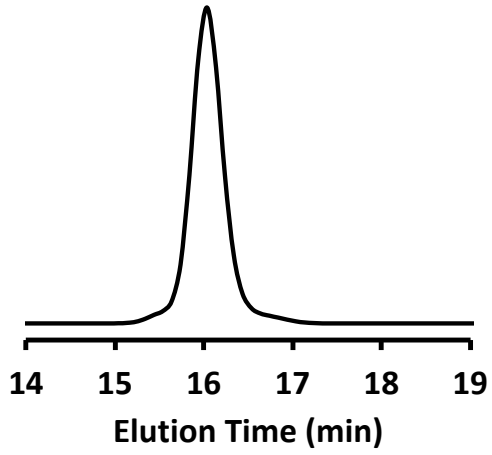

Fig. S14 SEC chromatogram of PS-$(OH)_2$-PMMA.

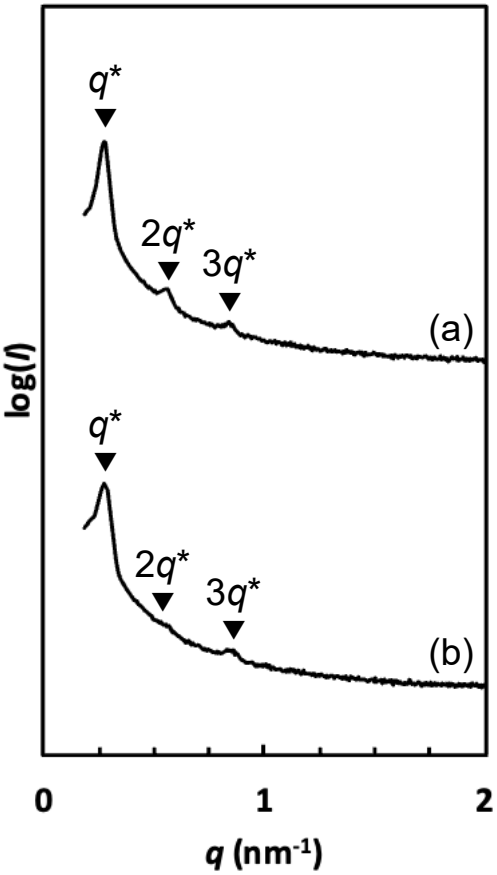

Fig. S15 1D SAXS profiles of (a) PS-$(OTBS)_2$-PMMA and (b) PS-$(OH)_2$-PMMA.

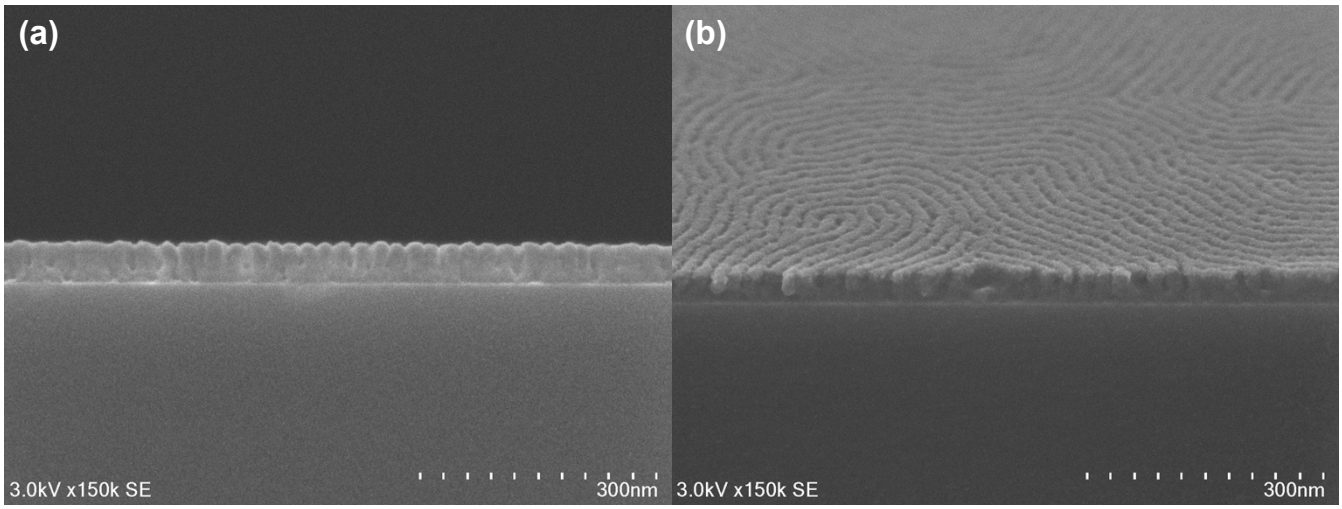

Fig. S16 (a) Cross-sectional and (b) tilted FE-SEM images of a PS-$(OH)_2$-PMMA thin film applied onto a PS-$(OH)_2$-PMMA neutral layer, which were annealed for 20 minutes. Both images were taken without the etching of PMMA domains.

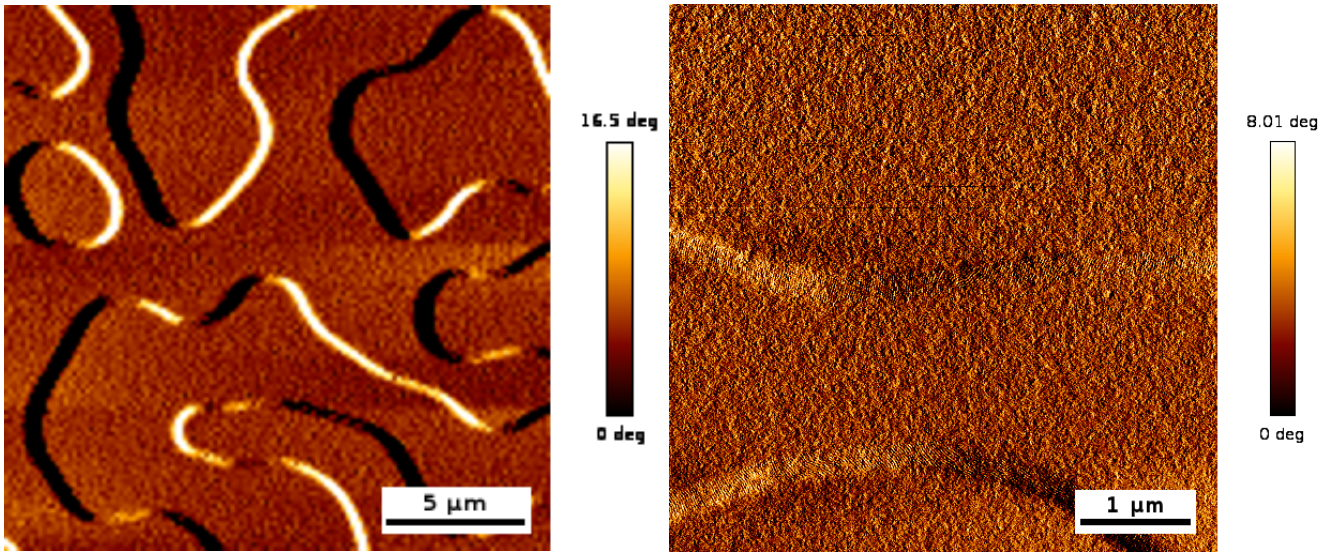

Fig. S17 AFM phase images (20 µm square, left, and 5 µm square, right) of PS-$(OH)_2$-PMMA thin films (~ 30 nm) applied onto a PS-$(OTBS)_2$-PMMA neutral layer annealed for 30 minutes, exhibiting parallel orientation of lamellae.

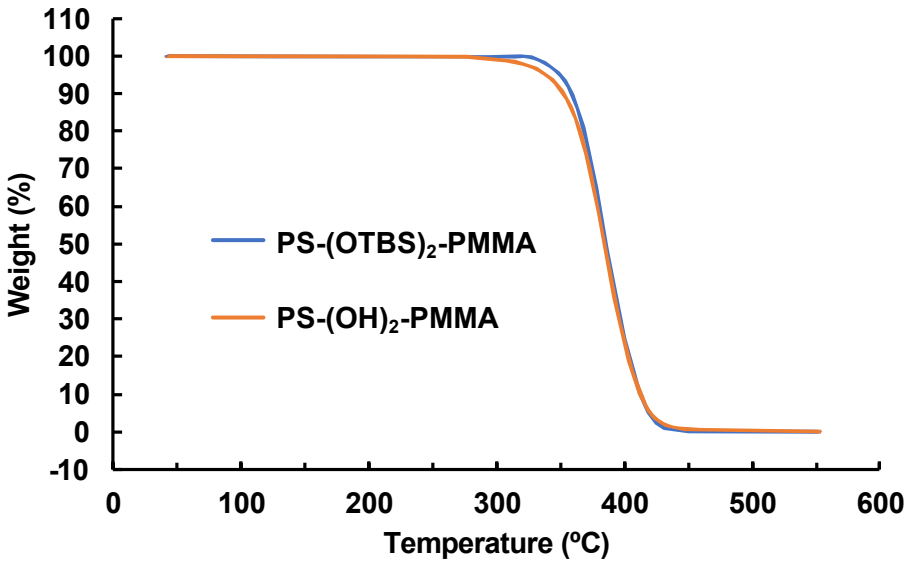

Fig. S18 TG curves of PS-$(OTBS)_2$-PMMA (blue line) and PS-$(OH)_2$-PMMA (orange line). 5% weight loss temperatures are 350ºC and 339ºC , respectively.

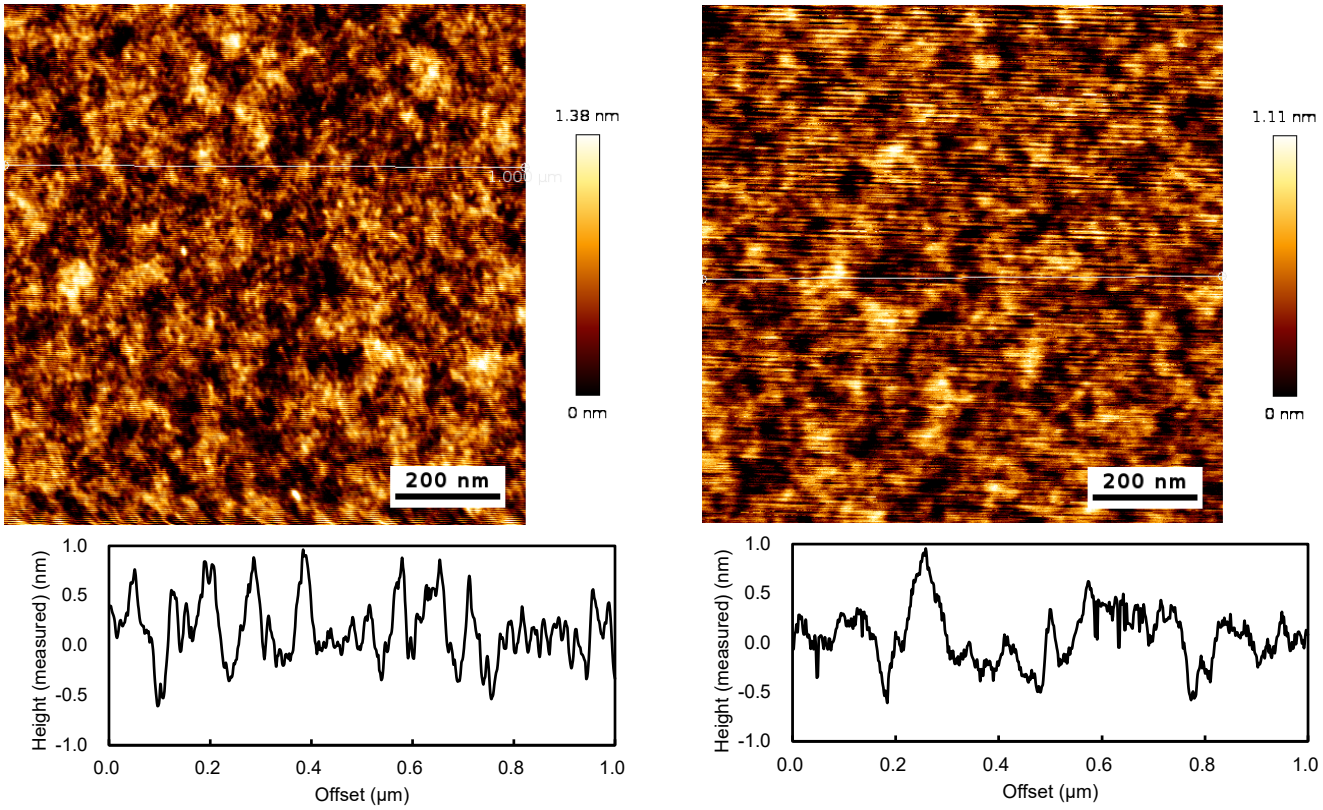

Fig. S19 AFM height images of PS-$(OH)_2$-PMMA neutral layers annealed for 1 minute (~ 6 nm, left) and 30 minutes (~ 8 nm, right), accompanied by the cross-sectional height profiles (taken from the white line in the images) below. The values of root-mean-square surface roughness of each NLs are 0.31 nm and 0.28 nm, respectively.

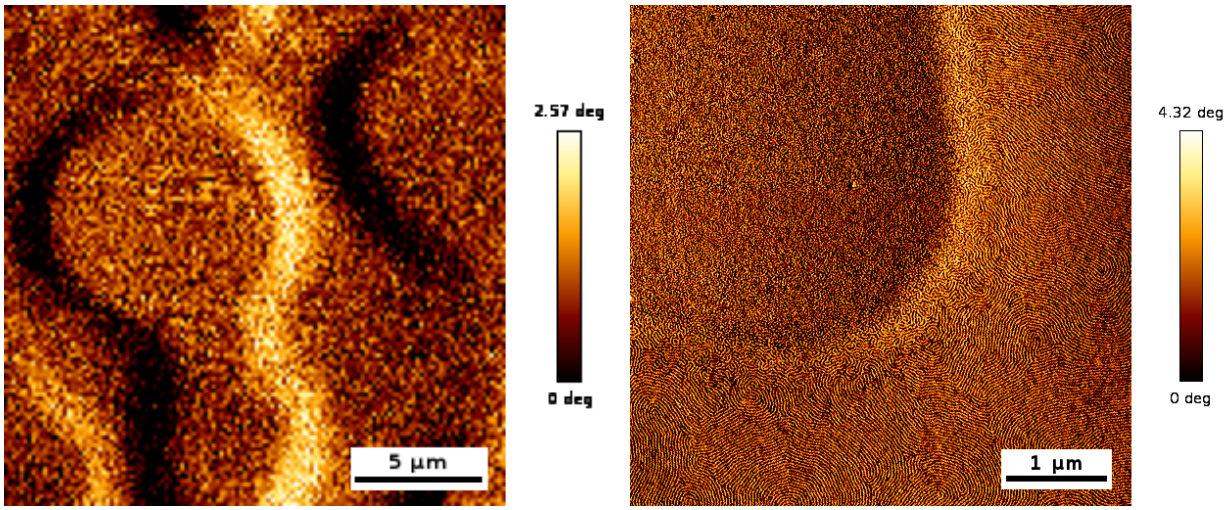

Fig. S20 AFM phase images of a PS-$(OH)_2$-PMMA thin film that were directly cast onto a Si substrate and annealed at 250ºC for 30 minutes (~ 40 nm). Perpendicular orientation of lamellae was only partly observed.

References

1 J. Wu, S. Bo, J. Liu, T. Zhou, H. Xiao, L. Qiu, Z. Zhen and X. Liu, *Chem. Commun.*, 2012, **48**, 9637-9639.